Similarity matrices as a new feature for acoustic emission analysis of concrete

Jochen H. Kurz, Florian Finck, Christian U. Grosse, Hans-Wolf Reinhardt
University Stuttgart, Institute for Construction Materials, Pfaffenwaldring 4, 70550 Stuttgart, Germany,
Phone: +49 - 711 - 6856792, Fax: +49 - 711 – 6856797

Abstract

The acoustic emission signal contains information about the fracture process which emits the signal and its travel path to the recording sensor. This is expressed in the signal's shape. Estimating the cross correlation function or the magnitude squared coherence function between several signals of clustered events, leads to information about the similarity of these signals, i.e. about the fracture processes and the travel paths. It is possible to use the signal's original shape or to calculate the envelope by the Hilbert transform or to use only a small window around the onset of the signal. With the help of a similarity matrix it is possible to investigate very quickly changes in the physical properties of the ray path of events from one cluster. I.e. changes concerning the dimension of the fracture area or internal stress redistributions become visible. The similarity analysis can be used to identify true acoustic emissions from artefacts and it can be used to reduce the number of events which must be localized to characterize the failure behaviour. Furthermore, the results can be surveyed by other fracture analysis procedures.

1. Introduction

The search for similarities in time series and the separation of clusters has been applied to many scientific areas, e.g. physics, biology, medicine and economy. The time series recorded in seismology and acoustic emission technique are caused by the same phenomenon: the sudden fracturing in a rigid body leads to the release of the stored elastic energy in form of elastic waves. The shape of these emitted elastic waves is influenced by the source-time function, the propagation path and the recording instruments. Conditions for similarity of the recorded signals are fulfilled if all contributing factors are essentially identical (Maurer and Deichmann, 1995).

A common approach in seismology for waveform matching, i.e. looking for similarities in the signals, is to calculate the cross-correlation function in the time domain (Thorbjanardottir and Pechman, 1987; Maurer and Deichmann, 1995; Schulte-Theis, 1995; Hemmann et al., 2003) or to calculate the cross-spectrum coherency function in the frequency domain (Poupinet et al., 1984; Aster and Rowe, 2000). In seismology waveform matching is a suitable approach for relative hypocenter localisation which leads to a much greater accuracy than the absolute localisation. E.g. if the events are situated outside the aperture of the recording network hypocenter determination relative to a master event leads to correct locations. Waveform matching is needed to define the events which due to their similarity belong to one cluster. Due to the factors which influence the shape of the signal (mentioned above), the events of one cluster are generally clustered in space and time.

Concerning acoustic emissions Grosse (1996), Grosse et al. (2004) and Köppel (2002) showed the applicability of the cross-spectrum coherency method for cluster separation. It will be shown in the following, that due to a significant similarity of certain signals, waveform matching of acoustic emissions (in frequency and in time domain) is able to reveal failure processes and to separate events clustered in space and time. Furthermore, the calculation of similarity matrices leads to images which are easy to interprete.

2. Cross correlation and cross-spectrum coherency

The cross-covariance function is one approach to describe the connection between

several stochastical processes. The normed cross-covariance is called cross-correlation and is defined as follows:

$$f(t) = \int_{-\infty}^{\infty} x(\tau)h(t+\tau)\,d\tau \qquad (1)$$

where x(τ) and h(τ) are two in our case time dependent functions and t denotes the displacement of one function relative to the other function along the time axis. The cross correlation function gives a measure of the similarity of two time series shifted along each other. The maximum value of f(t) indicates the maximum correlation of the two signals gained at the time shift t. Calculating the cross correlation function, the information about the phase is lost. I.e. it is not possible to calculate x(τ) and h(τ) from the cross correlation function (Buttkus, 1991).
The correlation of two functions in the frequency domain can be calculated by the cross-spectrum coherency function which is the Fourier transform of the cross correlation function. According Brigham (1974) this relation will be shown in the following:

$$\int_{-\infty}^{\infty} f(t)e^{-i2\pi\omega t}dt = \int_{-\infty}^{\infty}\left[\int_{-\infty}^{\infty} x(\tau)h(t+\tau)\,d\tau\right]e^{-i2\pi\omega t}\,dt \qquad (2)$$

After changing the order of integration:

$$F(\omega) = \int_{-\infty}^{\infty} x(\tau)\left[\int_{-\infty}^{\infty} h(t+\tau)e^{-i2\pi\omega t}\,dt\right]\,d\tau \qquad (3)$$

Applying the substitution $\sigma = t+\tau$ the term in square brackets can be written as:

$$\int_{-\infty}^{\infty} h(\sigma)e^{-i2\pi\omega(\sigma-\tau)}\,d\sigma \qquad (4)$$

$$\Longrightarrow \quad e^{i2\pi\omega\tau}\int_{-\infty}^{\infty} h(\sigma)e^{-i2\pi\omega\sigma}\,d\sigma \qquad (5)$$

$$\Longrightarrow \quad e^{i2\pi\omega\tau}H(\omega) \qquad (6)$$

where $H(\omega)$ is the Fourier transform of $h(t)$. Thus, equation (3) can be rewritten as:

$$F(\omega) = \int_{-\infty}^{\infty} x(\tau)e^{i2\pi\omega\tau}H(\omega)\,d\tau \qquad (7)$$

Equation (7) is equal to:

$$F(\omega) = H(\omega)\cdot X^*(\omega) \qquad (8)$$

where $X^*(\omega)$ is the complex conjugate of the Fourier transform of x(t). This compilation shows that the cross-spectrum coherency is the Fourier transform of the cross-correlation:

$$f(t) = \int_{-\infty}^{\infty} x(\tau)h(t+\tau)\,d\tau \iff F(\omega) = H(\omega)\cdot X^*(\omega) \qquad (9)$$

Concerning a discrete signal equation (9) is rewritten as:

$$f(kT) = \sum_{i=0}^{N-1} x(iT)h[(k+i)T] \iff F(\frac{n}{NT}) = X^*(\frac{n}{NT})H(\frac{n}{NT}) \qquad (10)$$

where N is the sample value, n are the number of sample intervals, T is the sample interval and k denotes the shift of the function $h(iT)$ by the amount kT.

Comparing all cross-correlation functions or cross-spectrum coherency functions gained from one dataset with each other does not provide eye-catching information. Therefore, the maximum of the cross correlation function f_{ij} normed by the auto-correlation function of

each time series f_{ii} and f_{jj} is calculated:

$$(XC)_{ij} = \frac{f_{ij}}{\sqrt{f_{ii} f_{jj}}} \qquad (11)$$

$$(fCC)_{ij} = max((XC)_{ij}) \qquad (12)$$

I.e. the correlation coefficient $(fCC)_{ij}$ is the maximum of $(XC)_{ij}$.
Concerning the cross-spectrum coherency function a similar parameter called magnitude squared coherence function is calculated (Carter and Ferrie, 1979):

$$(MSC)_{ij} = \frac{|F_{ij}|^2}{F_{ii} F_{jj}} \qquad (13)$$

$$(FCC)_{ij} = \frac{1}{n} \sum_{k=1}^{n} (MSC)_{ij,n} \qquad (14)$$

A correlation coefficient $(FCC)_{ij}$ for the magnitude squared coeherence function can be calculated by summing up the first n-values of the magnitude sqared coherence sequence which corresponds to the first n-frequencies of the spectrum. The number n has to be chosen according to the frequency range which should be investigated. Furthermore, the correlation coefficient is normed by number n of the chosen frequencies.

3. Application of the cross-correlation and the cross-spectrum coherency technique to acoustic emissions

The two methods for waveform matching described in the last section were applied to acoustic emission measurements of concrete. Different aspects were investigated which will be discussed in the following. Regarding the experiments, only a short description will be given, due to the fact that the tests are described in the literature in detail.
The first investigation concentrates on the change of energy of the signal's waveform by using the logarithm of its envelope (Wegler and Lühr, 2001). Herefore, two specimens of the same dimensions (100 mm x 300 mm x 300 mm) but one of steel fibre reinforced concrete (SFRC) and the other one of non-reinforced concrete (both specimens of concrete EN 206-1 C40/50) were tested. They were double-edge loaded and have been subjected to compressive loads. The aim of this test ist to get pure mode II failure. A detailed description of the experimental setup and the occurring fracture processes can be found in Reinhardt et al. (1997) and Reinhardt and Xu (1998).
The fiber reinforced concrete specimen showed significant failure due to the compressive load in the last quarter of the experiment. The crack path is mapped by the localized acoustic emissions (Fig. 1). Analyzing the change of the signals' energy by using the logarithm of the envelope, a break in the energy correlation expressed by the similarity matrix (Fig. 2) becomes visible.

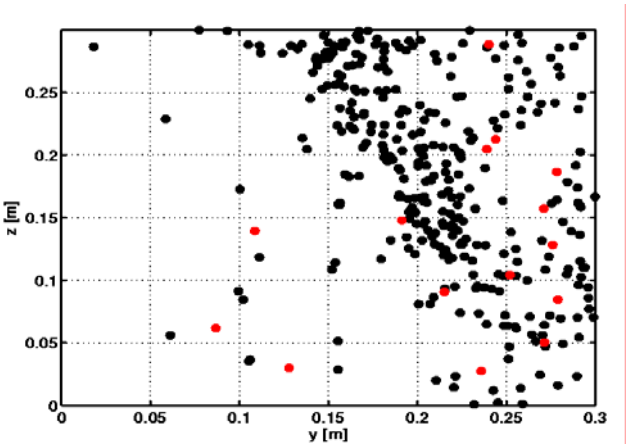

Fig.1. Localisation of the acoustic emissions generated during the test of the SFRC specimen. The red points are the localizable events with an event number greater than 3000.

The red colours in Fig. 2 indicate high correlation coefficients while the green and blue colours indicate low ones. Starting from approximately event 3200 the similarity decreases significantly. This was also the period where macroscopic visible cracks occurred on the surface of the specimen. The localization of the acoustic emissions confirms the behaviour of the waveforms of the signals. The red points in Fig. 1 are the localizable events with an event number greater than 3000. The result of the localization shows that only 4 % of the localizable events occurred in the last phase of the expeeriment. This is a further indicator that the failure of the specimen influences the waveform significantly.

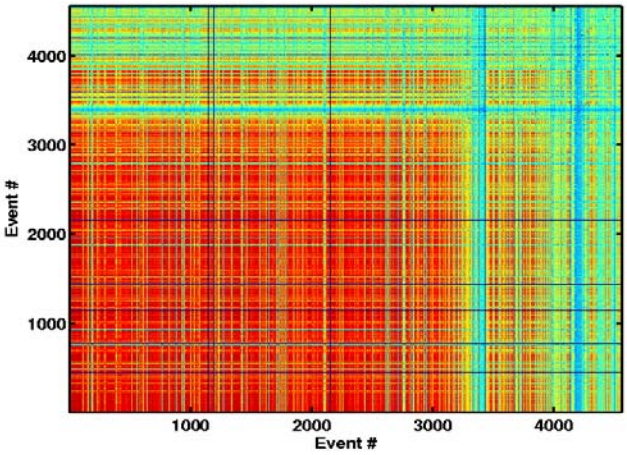

Fig. 2. Cross-correlation similarity matrix of the logarithmic envelope of all acoustic emission signals of the test of the SFRC specimen. I.e. not all recorded events were localizable, however the waveform itself could be used for investigations on waveform matching.

The similarity matrix of the non-reinforced specimen shows a similar behaviour as the SFRC specimen. However, the image does not contain such significant colour contrasts seperating the major fracture processes (Fig. 3). A huge red square ranging from approximately event 100 to event 700 marks the major fracture period where different fracture areas inside the specimen were activated but no significant macroscopic failure occurred. The first 100 events are uncorrelated events from the beginning of the test. The events which occurred in the last phase of the test (event 700 until end) belong to the state of compressive failure of the specimen. During this last phase macroscopic visible cracks occurred at the surface of the specimen, i.e. the waveforms were significantly influenced by the failure of the concrete.

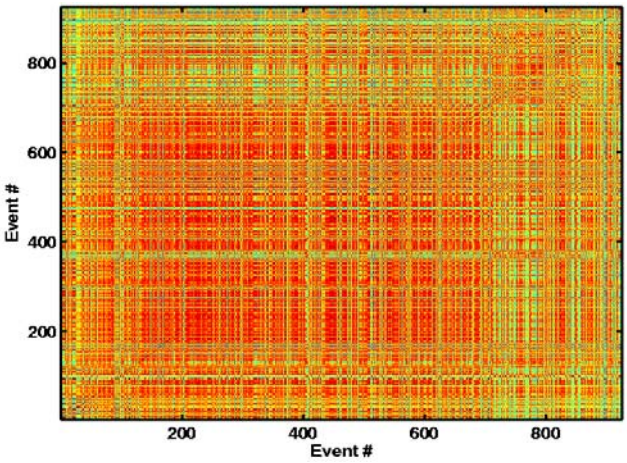

Fig. 3. Cross-correlation similarity matrix of the logarithmic envelope of all acoustic emissions from the test of the non-reinforced double egde loaded specimen.

The similarity matrix in Fig. 3 does not show very significant colour contrasts between the 3 major fracture periods. To check the significance of these 3 major clusters, a principal component analysis was performed. Herefore, the raw signals were taken, eigenvectors

and eigenvalues of the covariance matrix were calclated and finally the first two principal components using the eigenvectors and eigenvalues were determined. Fig. 4 shows the second principal component versus the first. The black points are the events 1 to 100, the red points are the events 101 to 700 and the green points are the events 701 to 932. The pricipal component analysis shows that the 3 major failure phases which are only weakly distinguishable in the similarity matrix (Fig. 3) can be separated clearly. I.e. the significance of the cluster separation in the similarity matrix is confirmed by the principal component analyis.

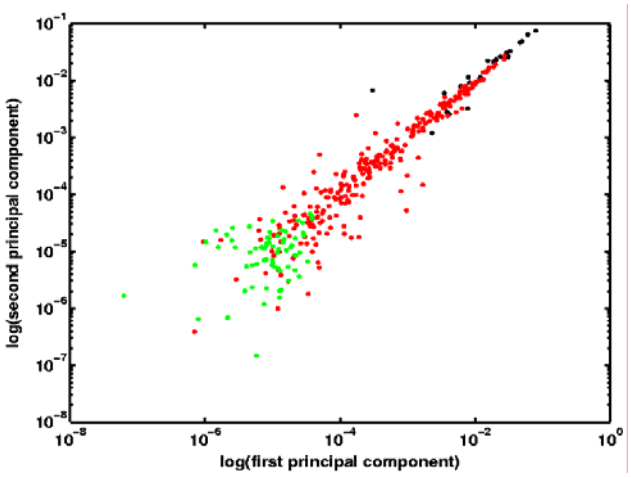

Fig. 4. Principal component analysis of the similarity matrix using only the eigenvectors and eigenvalues.

Looking at the distribution of certain acoustic emissions from one test, the cross-spectral coherency function leads to a good resolution of the clusters. Herefore, not the whole signal is taken, but a relative small window of about 100 samples around the onset of the signal. The length of the window is taken large enough that the first half wavelength of the signal is definitely within this window. Due to the fact that in general the events belonging to one cluster do not occurr all at once the similarity matrix gained after calculating the correlation coefficient of the magnitude squared coherency function (Equ. 14) has to be sorted. The chosen sorting algorithm is taking the euclidian norm of two rows or coloumns and defining a threshold for their similarity.
The sorted similarity matrix (coss-spectral coherency) of the acoustic emissions recorded during the test of the double edge loaded non-reinforced specimen mentioned above is shown in Fig. 5. The darker the red, the higher is the similarity coeffiecient. The corresponding colour coded localisation is shown in Fig. 6.

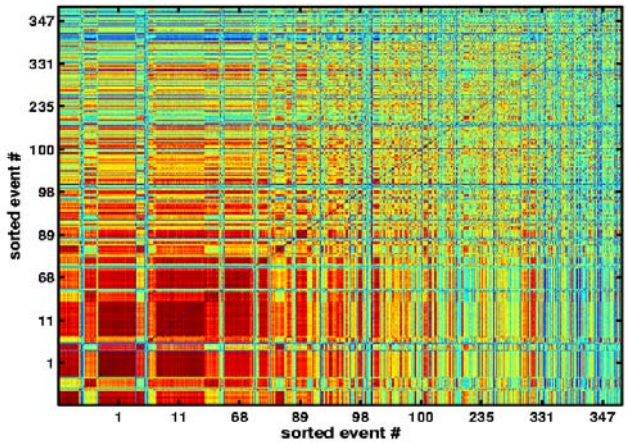

Fig. 5. Cross-spectral coherency similarity matrix of all acoustic emissions from the test of the non-reinforced double egde loaded specimen.

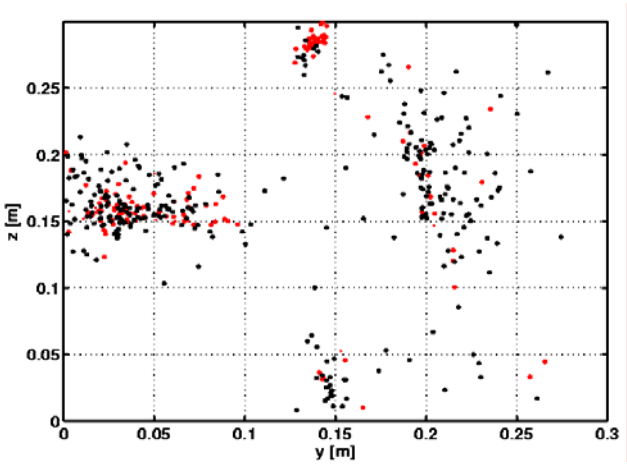

Fig. 6. Localisation of the acoustic emissions. The red events are the events of the 4 huge dark red squares of the left graph which are similar to each other.

The events belonging to the 4 largest dark red squares of Fig. 5 are displayed in red in Fig. 6. All other localizable events from the test are displayed in black. The similarity matrix shows that there is not only a high similarity in the 4 largest clusters but also between these clusters. This implies that the events take place in close proximity in order to fulfill the condition that the elastic waves follow similar ray-paths between hypocenter and sensor. They must also have similar source-time functions which implies that they should be in approximately the same amplitude range. The localization of these events shows that the main part of the cluster at top middle position and the central part of the cluster in the middle of the left hand side are represented by the events belonging to the 4 largest clusters of Fig. 5. The existence of the two other clusters (bottom middle and right hand side) is only indicated. Concerning the focal mechanism the events at top middle and bottom middle position represent mode II failure and the events in the middle of the left hand side represent mode I failure. The different fracture modes could not be distinguished by the cross-spectral coherency approach. However, especially the two largest clusters of Fig. 5 contain events with low localization errors which furthermore represent the kernel of the four failure areas. I.e. it was possible to seperate a minimum number of events by the cross-spectral coherency similarity matrix which characterize the fracture behaviour of the test specimen.

4. Conclusion

The waveform of acoustic emissions contains information about the ray-paths of the elastic waves and about the source type function. Using the cross-correlatin function of the logarithmic envelope of the signals, material changes due to failure processes along the ray-path could be visualized. Both double edge loaded test specimens (the one with steel fibre reinforcement and the non-reinforced one) show failure under compressive load during the last quarter of the experiment. This behaviour is also reflected by the similarity matrices. They show a significant decrease in the similarity coefficients (Fig. 2 and Fig. 3) of the events which occurred in the last quarter of the test. It could be shown that macrosopic fractures strongly influence the waveform of the acoustic emissions.
The cross-spectral coherency analysis is able to separate a minimum number of events which characterizes the complete fracture behaviour of the test specimen.
Concerning structural health monitoring both procedures can help in event classification and in data reduction that only relevant acoustic emissions are used for further investigations.

5. Acknowledgements

This work was carried out in the collaborative research centre SFB 381 at the University Stuttgart whose financial support by the Deutsche Forschungsgemeinschaft is gratefully acknowledged.

6. References

Aster, R., Rowe, C., 2000. Automatic phase pick refinement and similar event association in large seismic datasets. Kluwer Academic Publishers, Netherlands, CH.9. pp. 231 – 263.

Brigham, E., 1974. The fast fourier transform. Prentice-Hall, Inc., Englewood Cliffs, USA.

Buttkus, B., 1991. Spektralanalyse und Filtertheorie in der angewandten Geophysik. Springer Verlag, Berlin Heidelberg.

Carter, C., Ferrie, J.F., 1979. A Coherence and Cross Spectral Estimation Program. IEEE Press, Ch. 2.3.

Grosse, C.U., Finck, F., Kurz, J.H. Reinhardt, H.-W., 2004. Improvements of AE technique using wavelet algorithms, coherence functions and automatic data analysis. Construction and Building Materials 18, 203 – 213.

Grosse, C.U., 1996. Quantitative zerstörungsfreie Prüfung von Baustoffen mittels Schallemissionsanalyse und Ultraschall. Ph.D. Thesis, Universität Stuttgart.

Hemmann, A., Meier, T., Jentzsch, G., Ziegert, A., 2003. Similarity of waveforms and relative relocalisation of the earthquake swarm 1997/1998 near Werdau. Journal of Geodynamics 25 (1-2), 191 – 208.

Köppel, S., 2002. Schallemissionsanalyse zur Untersuchung von Stahlbetontragwerken. Ph.D. Thesis, ETH Zürich.

Maurer, H., Deichmann, N., 1995. Microearthquake cluster detection based on waveform similarities, with an application to the western Swiss Alps. Geophysical Journal International 123, 588 – 600.

Poupinet, G., Ellsworth, W., Frechet, J., 1984. Monitoring velocity variations in the crust using earthquake doublets: an application to the Calaveras Fault, California. Journal of Geophysical Research 89 (B9), 5719 – 5731.

Reinhardt, H.-W., Ozbolt, J., Xu, S., Dinku, A., 1997. Shear of Sructural Concrete Members and Pure Mode II Testing. Advanced Cement Based Materials 5, 75 – 85.

Reinhardt, H.-W., Xu, S., 1998. Experimental determination of K_{IIc} of normal strength concrete. Materials and Structures 31, 296 – 302.

Schulte-Theis, H., 1995. Automatische Lokalisierung und Clusteranalyse regionaler Erdbeben. Ph.D. Thesis, Ruhr-Universität Bochum.

Thorbjanardottir, B., Pechman, J., 1987. Constraints on relative earthquake locations from crosscorrelation of waveforms. BSSA 77, 1626 – 1634.

Wegler, U., Lühr, B.G., 2001. Scattering behaviour at Merapi volcano (Java) revealed from an active seismic experiment. Geophysical Journal International 145, 579 – 592.